

BCSJ Award Article

Visible Light-Induced Electron Transfers in Titania Nanosheet and Mesoporous Silica Integrated Films

Tatsuto Yui,[1,3] Takako Tsuchino,[1] Kosho Akatsuka,[2] Atsushi Yamauchi,[1] Yuka Kobayashi,[1] Takeshi Hattori,[1] Masa-aki Haga,[2,3] and Katsuhiko Takagi*[1,3]

[1]Department of Crystalline Materials Science, Graduate School of Engineering, Nagoya University, Furo-cho, Chikusa-ku, Nagoya 464-8603

[2]Department of Applied Chemistry, Faculty of Science and Engineering, Chuo University, 1-13-27 Kasuga, Bunkyo-ku, Tokyo 112-8551

[3]CREST (JST)

Received September 22, 2005; E-mail: ktakagi@apchem.nagoya-u.ac.jp

Two spatially different nano-structured inorganic materials, titania nanosheets (TNS) and mesoporous silica (MPS), were integrated onto a glass substrate to form stacked composite thin films. Investigations were then carried out on photoinduced electron transfers between the tetrakis(1-methylpyridinium-4-yl)porphyrinatometal(4+) ion ([M(tmpyp)]$^{4+}$); M = H_2, Zn, and Co) and 1,1′-dimethyl-4,4′-bipyridinium (methyl viologen; MV^{2+}) within the hybrid films. The [M(tmpyp)]$^{4+}$ molecules were found to be adsorbed only in the MPS nano-cavities, while MV^{2+} was intercalated only in the TNS layer, i.e., the [M(tmpyp)]$^{4+}$ and MV^{2+} molecules could be separately and selectively accommodated into the MPS nano-cavities and TNS layers of the hybrid films, respectively. Upon UV light irradiation (TNS excitation) of the films containing [H_2(tmpyp)]$^{4+}$, the decomposition of [H_2(tmpyp)]$^{4+}$ and the formation of a one-electron reduced MV^{2+} ($MV^{+\bullet}$) were observed, clearly indicating photoinduced electron transfers in the MPS/TNS films. Moreover, when the metal-complex [Zn(tmpyp)]$^{4+}$ or [Co(tmpyp)]$^{4+}$ was used in place of [H_2(tmpyp)]$^{4+}$, visible light-induced electron transfers could be observed in the present MPS/TNS hybrid films, the first report of such charge separation in consecutively stacked thin films by visible light.

The hybridization of organic compounds and nano-structured inorganic compounds, such as zeolites, mesoporous silicas, and layered inorganic compounds, have been the focus of many studies in recent years.[1–9] Hybridization with photonically active organic molecules are of special interest due to their characteristic photochemical and photophysical properties, which can be applied in the design of photofunctional materials and systems.[6,8,9]

Mesoporous silicas (MPS), such as MCM-41 and FSM-16, are known to have regularly-oriented cavities of only a few nanometers and various chemical species can be incorporated within these nano-cavities.[5,6] The incorporated molecules also exhibit unique behavior attributed to the interactions that occur between the adsorbed molecules and nano-cavities. MPS are therefore of great interest as adsorbents, molecular sieves, reaction vessels, and reaction fields.[1,2,5,6]

Layered inorganic compounds, such as clay minerals, layered double hydroxides, and layered metal-oxide semiconductors (LMOS), have structures of stacked nano-sized inorganic plates so that they are able to accommodate organic guests within their interlayers.[7–10] It is known that the intercalated molecules may orient themselves in an ordered alignment due to the electrostatic interaction between the inorganic layers and the interactions between the adsorbed molecules.[8–10] Among these compounds, LMOSs are especially interesting since they not only have a layered structure, but also exhibit photocatalytic activity.[8,9] Thus, various studies of the photochemical electron transfers between LMOS and organic dyes in hybridized systems and their application to visible light-responsive photocatalysts are being carried out.[8,9,11–15]

The photoinduced electron transfers between porphyrins[16] and 1,1′-dimethyl-4,4′-bipyridinium (methylviologen; MV^{2+}) through LMOS as the model system have been previously reported,[15] and we have observed very unique photochemical behavior when, compared with reactions in homogeneous solutions[16–18] or on the surface of TiO_2 particles.[19,20] We have aimed for an improvement in the photoinduced electron transfers as well as the suppression of back electron transfers by the proximate and regular orientation of the porphyrins as the sensitizer and MV^{2+} as the electron acceptor within these LMOS layers. In fact, light-induced electron transfers between the porphyrins and MV^{2+} could be observed for the porphyrin/

Published on the web March 8, 2006; DOI 10.1246/bcsj.79.386

$TiNbO_5/MV^{2+}$ triad systems. These findings showed that the $TiNbO_5$ layers work as effective charge transporters and charge-separation mediators.[15] However, many powdered LMOS compounds, such as $K_4Nb_6O_{17}$ and $KTiNbO_5$, are inferior due to the lack of expandability in the layers caused by the high surface charge density. This leads to disadvantages for powdered LMOS such as limitations in the amount of molecules that can be adsorbed, inefficient dispersion in ordinary solvents, and a lack of transparency.

Meanwhile, titania nanosheets (TNS) developed by Sasaki et al.[9a,21–25] were seen to exhibit a complete exfoliation of the layered titanate crystals of several micrometers diameter and 0.45 nm thickness in aqueous dispersion. These TNS exhibited good dispersion as well as transparency in solvents, and at the same time, the ability of hybridization with various cationic molecules.[9,21–26] In line with this work, we have reported on the synthesis of transparent TNS thin films by electrophoretic deposition and their photocatalytic reactivity.[27] However, the selective and regular orientation of several different species in the TNS layers was difficult due to their nonselective homogeneous dispersion in solution.

Here, we have focused on integrated hybrid films of titania nanosheets (TNS) and mesoporous silica (MPS).[28] Using two structurally different types of uniquely-oriented inorganic host materials, i.e., the MPS cavities and the TNS interlayers, the closely-packed and regularly-oriented accommodation of two organic guest compounds, $[M(tmpyp)]^{4+}$ and MV^{2+}, could be carried out separately and selectively. Moreover, photoinduced electron transfers between the porphyrins and methyl viologens through the TNS layers could be initiated in these hybrid films. This work presents the synthesis of these MPS/TNS hybrid films, analysis of the closely-packed and regular orientation of the porphyrins and MV^{2+}, as well as studies of photoinduced electron transfers that could be initiated in these hybrids both by UV and visible light. The molecular formula of the metalloporphyrin derivatives (tetrakis(1-methylpyridinium-4-yl)porphyrinatometal(4+) ion ($[M(tmpyp)]^{4+}$); M = H_2, Zn, and Co) and MV^{2+} are shown in Chart 1. The composition of the hybrid films, $([M(tmpyp)]^{4+}$–MPS)/(MV^{2+}–TNS), indicates that the MV^{2+}-adsorbed TNS films are consecutively stacked on the $[M(tmpyp)]^{4+}$-adsorbed MPS films. A schematic drawing of the MPS/TNS hybrid in Fig. 1 shows the $[M(tmpyp)]^{4+}$ and MV^{2+} molecules to be separately accommodated in MPS and TNS, respectively.

Experimental

Materials. Tetramethoxysilane (TMOS; TCI), tetrabutylammonium hydroxide (TBA^+ OH^-; Aldrich), 1,1′-dimethyl-4,4′-bipyridinium (methylviologen dichloride; MV^{2+} $2Cl^-$, TCI), cetyltrimethylammonium chloride (CTAC; TCI), hydroquinone (HQ; TCI), and methylene blue (MB; TCI) were used as received.

$[H_2(tmpyp)]^{4+}$ tetrakis(1-methylpyridinium-4-yl)porphyrin(4+) ion *p*-tosylate salt (TCI) of extra pure grade was used without further purification. $[Zn(tmpyp)]^{4+}$ and $[Co(tmpyp)]^{4+}$ were synthesized from $[H_2(tmpyp)]^{4+}$ according to procedures reported in previous literature.[29,30]

The protonated titanate ($H_{0.7}Ti_{1.825}\square_{0.175}O_4 \cdot H_2O$), as the precursor of TNS, was prepared by procedures reported by Sasaki et al.,[21–23] and the structures were confirmed by X-ray diffraction analysis (XRD).[27] The obtained protonated titanate (1.2 g) was shaken vigorously with 33 mM of a TBA^+ OH^- aqueous solution (100 mL), which corresponded to 0.7 equiv of the anionic sites of TNS, for 2 weeks at ambient temperature, leading to exfoliated titania nanosheets (TNS) in a colorless turbid solution.[21–23]

Synthesis of the ($[M(tmpyp)]^{4+}$–MSP)/(MV^{2+}–TNS) Hybrid Thin Films. The synthesis of the ($[M(tmpyp)]^{4+}$–MSP)/

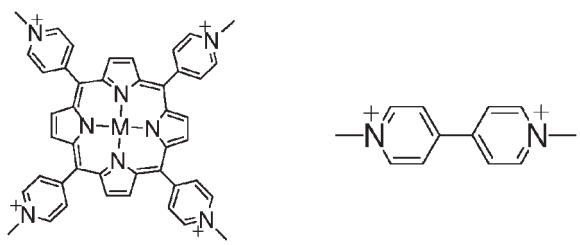

Chart 1.

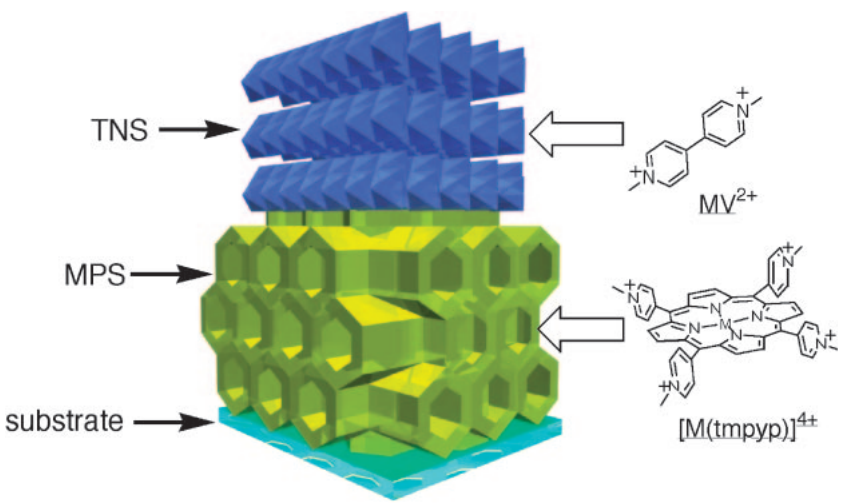

Fig. 1. Schematic structure of the ($[M(tmpyp)]^{4+}$–MPS)/(MV^{2+}–TNS) hybrid films.

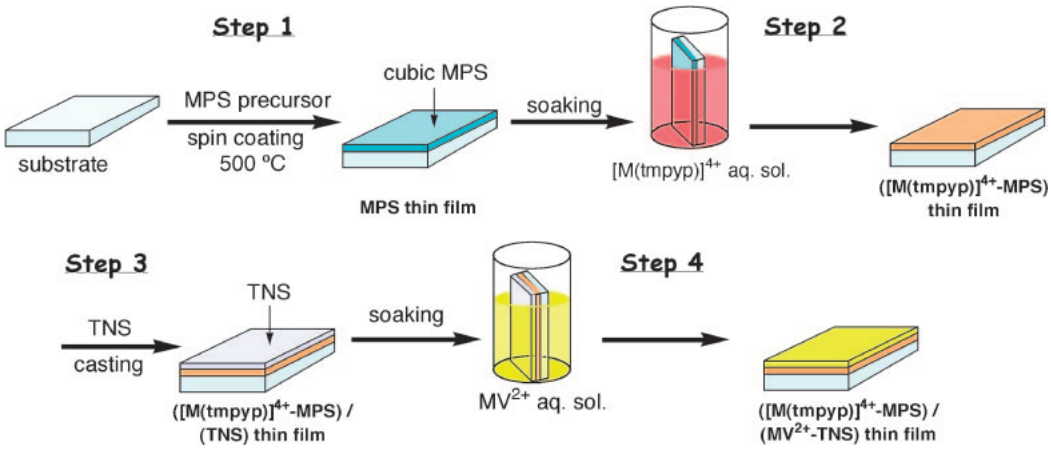

Scheme 1.

(MV^{2+}–TNS) hybrid films is outlined in Scheme 1.[28]

Step 1. Preparation of the MPS Film: An aqueous MPS precursor gel mixed with the cationic surfactant, i.e., CTAC and TMOS, was spin-coated (3000 rpm, 10 s) on a quartz substrate ($2 \times 2\,cm^2$) and then calcinated at 500 °C for 3 h under a flow of air.[31] Three characteristic XRD signals showed the resulting transparent mesoporous silica (MPS) thin films to be cubic in structure with a regularity of the d_{210} distance at 3.34 nm and a pore size of 2.1 nm.[31] The obtained MPS films were then treated with a 0.1% NaOH in methanol solution for 1 min at room temperature (rt), washed well with methanol and dried at ca. 70 °C for a few minutes.[5a,b]

Step 2. Adsorption of $[M(tmpyp)]^{4+}$ in MPS: The MSP thin films were then soaked in a $[M(tmpyp)]^{4+} = 9.7 \times 10^{-5}$ M aqueous solution for 1 h at rt, washed well with water, and dried under ambient atmosphere. Brownish and transparent ($[M(tmpyp)]^{4+}$–MPS) films were obtained. $[M(tmpyp)]^{4+}$ was found to be adsorbed in the MPS nano-cavities and the adsorbed amounts of $[M(tmpyp)]^{4+}$ (5.2×10^{-7} mol g^{-1}) were estimated from the absorption measurements of the residual solution. As judged by the surface area of MPS (920 m^2 g^{-1}),[31b] the average occupational area of one $[M(tmpyp)]^{4+}$ molecule was estimated to be 2900 nm^2.

Step 3. Integration of the TNS Films: A 0.4 wt % aqueous dispersion of TNS was cast onto the ($[M(tmpyp)]^{4+}$–MPS) thin films, kept standing for 24 h, and dried under ambient atmosphere to obtain the ($[M(tmpyp)]^{4+}$–MPS)/(TNS) films.

Step 4. Intercalation of MV^{2+} in TNS: The ($[M(tmpyp)]^{4+}$–MPS)/(TNS) films were then soaked in a $[MV^{2+}] = 2.1 \times 10^{-4}$ M aqueous solution at rt for 4 h and dried in vacuo. Brownish and transparent ($[M(tmpyp)]^{4+}$–MPS)/(MV^{2+}–TNS) thin films were formed. Approximately 30% of the cation exchange sites in the TNS interlayers were occupied by MV^{2+}.[27] However, a control experiment showed that the MV^{2+} molecules were not adsorbed into the MPS nano-cavities. This may be a result of the strong hydrophilicity of the MV^{2+} molecules as well as the incompatibility of the molecular size of MV^{2+} and the pore size of the MPS nano-cavities. However, it was observed that the MV^{2+} molecules did not transfer within the MPS or ($[M(tmpyp)]^{4+}$–MPS) hybrid films by the insertion of a third solid film between the MV^{2+}–TNS and $[M(tmpyp)]^{4+}$–MPS films, although more detailed experiments under various conditions are now underway. The fact that there was no transfer of the MV^{2+} in TNS may be understood not only by the high hydrophilic nature of the MV^{2+} molecules, but also by the large difference in size between the MV^{2+} molecules and the MPS pores. In fact, it has been reported that the pores of MPS and the molecules of the guests sensitively discriminate so that adsorption takes place only when the sizes are optimal, thus reflecting the adsorption efficiency.[5a,b] To prevent the MV^{2+} from migrating into the MPS nano-cavities, the (MV^{2+}–TNS) film was first independently prepared and the ($[H_2(tmpyp)]^{4+}$–MPS) hybrid fine film was then cast onto the (MV^{2+}–TNS) film without immersing the hybrid substrate into the MV^{2+}–TNS suspension. The UV light-induced electron transfers observed in the present carefully prepared hybrid film clearly indicate that MV^{2+} was not included within the MPS nano-cavities, therefore, the electron transfers seen here were not due to the codissolved $[H_2(tmpyp)]^{4+}$ and MV^{2+} within the nano-cavities.

Co-Adsorption of Hydroquinone (HQ) and Methylene Blue (MB): In order to introduce the sacrificial reductant into the hybrid films, the co-adsorption of HQ or MB with $[H_2(tmpyp)]^{4+}$ in the MPS nano-cavities was carried out in place of Step 2 by the following procedures: The MPS films were soaked in a mixture of $[M(tmpyp)]^{4+} = 1.1 \times 10^{-4}$ M and $[HQ] = 1.1 \times 10^{-3}$ M or $[MB] = 6.4 \times 10^{-5}$ M aqueous solution for 1 h at rt, washed well with water and then dried in vacuo. The [(HQ or MB + $[H_2(tmpyp)]^{4+}$)–MPS]/(MV^{2+}–TNS) hybrid films were then prepared following the procedures for Steps 3 and 4. After these steps, no desorption for the HQ or MB molecules could be confirmed by absorption spectral analysis of the hybrid films.

UV and Visible Light Irradiation. The ($[M(tmpyp)]^{4+}$–MSP)/(MV^{2+}–TNS) hybrid films were irradiated with a 300 W Xe lamp (XDS-301S, WACOM, Co.) as the light source at a distance of 10 cm under an aerated atmosphere. A combination of two cut-off filters, UTVAF-50S and -43U (HOYA), was used for UV light irradiation of 270–380 nm. Under these conditions, TNS was seen to function as a photocatalyst since almost all of the incident light (>99%) was absorbed by the TNS. A combination of two glass filters, B-460 and L-39 (HOYA), was used for visible light irradiation of 390–550 nm in order to selectively excite the porphyrin molecules. The absorption spectra were then measured as a function of the irradiation time.

Equipment. Scanning electron micrograph (SEM) images were recorded on a JSM-5600 apparatus (JEOL) operating at 20 kV for the Au-coated samples. Powder X-ray diffraction analysis (XRD) was carried out with a Rigaku RINT-2100 XRD apparatus operating at 40 kV and 40 mA and set at Ni-filtered Cu Kα radiation of 0.154 nm wavelength. The UV–visible absorption spectra were recorded in the transmittance mode with a JASCO

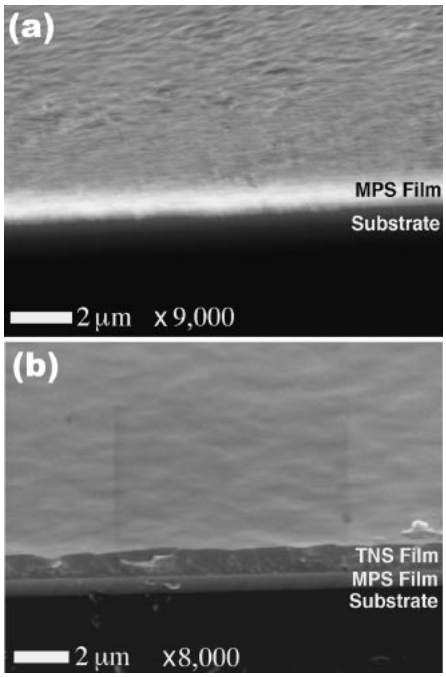

Fig. 2. Cross-sectional SEM images of: (a) the MPS film and; (b) the ($[H_2(tmpyp)]^{4+}$–MPS)/(MV^{2+}–TNS) hybrid film, on a quartz substrate.

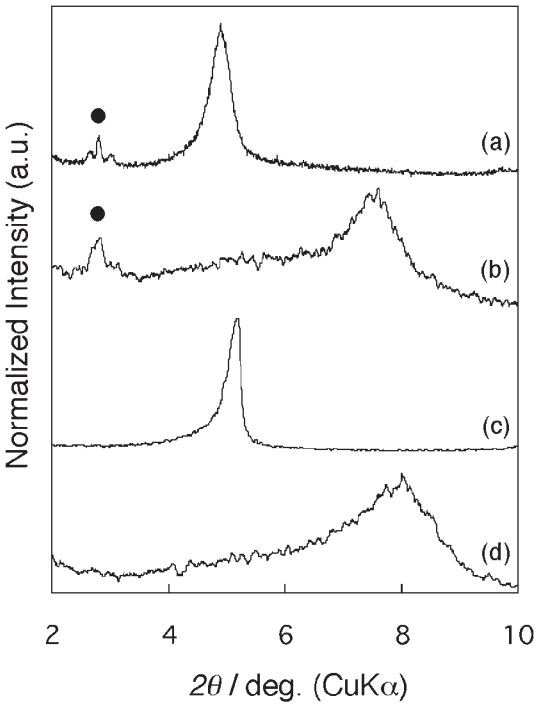

Fig. 3. XRD profiles of four different films: (a) the ($[H_2(tmpyp)]^{4+}$–MPS)/(TNS) films before soaking in MV^{2+} solution; (b) the ($[H_2(tmpyp)]^{4+}$–MPS)/(MV^{2+}–TNS) films after soaking in MV^{2+} solution; (c) the TNS cast films alone without MSP; and (d) the (c) film soaked in MV^{2+} solution (MV^{2+}–TNS film). Solid circles indicate the diffractions of the MPS nano-cavities.

type V-550 spectrometer. The fluorescence spectra were recorded on a JASCO FP-750 fluorescence spectrophotometer.

Results and Discussion

Structural Analysis of the Hybrid Films. The structures of the mesoporous silica/titania nanosheet [(MPS)/(TNS)] hybrid films were analyzed by scanning electron micrograph (SEM) and X-ray diffraction (XRD) investigations. The cross-sectional SEM images of the MPS film (Step 1) and the ($[H_2(tmpyp)]^{4+}$–MPS)/(MV^{2+}–TNS) hybrid film (Step 4) are shown in Figs. 2a and 2b, respectively. A uniform MPS thin film formation on the quartz substrate having a thickness of ca. 0.8 μm can be seen in Fig. 2a. Moreover, ($[H_2(tmpyp)]^{4+}$–MPS)/(MV^{2+}–TNS) exhibits a clear [substrate–MPS–TNS] tri-layer structure (Fig. 2b), and the estimated film thickness of TNS was calculated to be ca. 1.2 μm. MPS and TNS were thus observed to be independently stacked on the substrate without any peel off or disorientation of the films, even during the experimental procedures (Steps 1–4).

XRD analysis indicated a clear $d_{210} = 3.34$ nm diffraction peak due to the cubic structure of MPS, which remained unchanged during the soaking procedure in the $[M(tmpyp)]^{4+}$ aqueous solution (Step 2). The *cubic* mesopore structures were thus seen to remain unchanged by soaking in water or adsorption of $[M(tmpyp)]^{4+}$. The XRD profiles of the ($[H_2(tmpyp)]^{4+}$–MPS)/(TNS) (Step 3) and ($[H_2(tmpyp)]^{4+}$–MPS)/(MV^{2+}–TNS) (Step 4) hybrid films, the TNS cast film without MPS, and the (MV^{2+}–TNS) film[27] are shown in Figs. 3a–3d.

Two characteristic diffraction peaks were observed for the ($[H_2(tmpyp)]^{4+}$–MPS)/(TNS) hybrid film, as shown in Fig. 3a. The diffraction peak at $2\theta = 2.8$ deg. attributed to MPS can be seen to remain unchanged when compared to the original MPS films, even after the casting of the TNS dispersion (Step 3). However, the $2\theta = 4.9$ deg. (1.74 nm) peak was similar to that of the TNS cast films (Fig. 3c), indicating the stacked arrangement of the TNS films incorporated with TBA^+ molecules in their interlayers.[27] After soaking in an MV^{2+} aqueous solution (Fig. 3b; Step 4), the diffraction peak of TNS shifted to higher regions in a similar manner to the (MV^{2+}–TNS) films (Fig. 3d).[27] The TBA^+ molecules in the TNS interlayers were substituted with MV^{2+} and the MPS cubic mesopore structure could be retained, even after soaking in an MV^{2+} aqueous solution.

Adsorption of $[M(tmpyp)]^{4+}$ into the MPS Nano-Cavities. The selective adsorption of $[M(tmpyp)]^{4+}$ into the MPS nano-cavities was also investigated. There have been reports of the leveling or flattening of the methylpyridinium moieties of $[M(tmpyp)]^{4+}$ that induce a gradual red-shift of the $[M(tmpyp)]^{4+}$ Soret absorption band with the adsorption on the surface or interlayers of the inorganic layered sheets.[32–34] In fact, Inoue et al. have reported that $[M(tmpyp)]^{4+}$ (M = H_2 and Zn) exhibits an extreme red-shift when adsorbed on layered clay minerals.[33,34] That is, when the $[M(tmpyp)]^{4+}$ molecules are adsorbed on an exfoliated clay sheet, the absorption maximum shows a red-shift of ca. 30 nm compared to aqueous solution. Moreover, when the $[M(tmpyp)]^{4+}$ molecules were intercalated within the stacked clay interlayers, a 50–60 nm red-shift compared to the aqueous solution was observed due to the gradual leveling or flattening of the methylpyridinium ring. The adsorbed state of $[M(tmpyp)]^{4+}$ was estimated by

Table 1. Soret Absorption Maxima (nm) of $[M(tmpyp)]^{4+}$ in Various Systems

System	$[M(tmpyp)]^{4+}$		
	H_2	Zn	Co
(A) aq. sol.	421	435	428
(B) ($[M(tmpyp)]^{4+}$–MPS)	430	445	438
(C) ($[M(tmpyp)]^{4+}$–MPS)/(TNS)	433	450	441
(D) ($[M(tmpyp)]^{4+}$–MPS)/(MV^{2+}–TNS)	433	450	441
(E) ($[M(tmpyp)]^{4+}$–TNS)	475	462	462
(F) Surface adsorption on clay[a)]	451.5	462.5	—
(G) Intercalation in clay layer[a)]	484.5	486.0	—

a) Reported value in Ref. 33b.

analysis of the Soret absorption maxima and the absorption spectra were measured under the following conditions: (A) in aqueous solution; (B) within the ($[M(tmpyp)]^{4+}$–MPS) thin films (Step 2); (C) in the ($[M(tmpyp)]^{4+}$–MPS)/TNS films (Step 3); (D) in the ($[M(tmpyp)]^{4+}$–MPS)/(MV^{2+}–TNS) films (Step 4); (E) in the ($[M(tmpyp)]^{4+}$–TNS) cast film; (F) for the surface adsorbed on a single saponite clay sheet; and (G) within the saponite clay interlayers.[33b] The Soret absorption maxima of $[M(tmpyp)]^{4+}$ for these seven different systems are summarized in Table 1.

The absorption maxima for the Soret band of $[M(tmpyp)]^{4+}$ in MPS for all the systems from B to D showed a red-shift of 9–15 nm, compared to those in aqueous solution. The Soret band maxima of the porphyrins are known to be sensitive to the polarity of the solvent used, i.e., in a less polar solvent environment, the absorption maximum shifts toward longer wavelengths.[10f] The observed red-shift indicates a decrease in the polarity of the environment surrounding $[M(tmpyp)]^{4+}$ within the MPS nano-cavities. However, for the layered systems, TNS and clay systems E–G, the Soret bands showed significant red-shifting (27–63 nm) compared to the aqueous solution. Spectroscopic investigations showed the adsorbed $[M(tmpyp)]^{4+}$ molecules to be level or flat against the TNS layer similar to porphyrins incorporated in layered clay systems F and G. The Soret absorption maxima of $[M(tmpyp)]^{4+}$ for MPS systems B–D were observed to be different from those for the TNS or clay systems E–G. These results showed that $[M(tmpyp)]^{4+}$ is not affected by the procedures in Steps 3 and 4, and that the porphyrins were adsorbed only in the MPS nano-cavities and not intercalated into the TNS layers. Moreover, the fluorescence spectra of the porphyrins showed dramatic changes, i.e., a substantial broadening and change in the spectral shape due to the formation of molecular aggregates. However, the emission spectra of $[M(tmpyp)]^{4+}$ in MPS were similar to those for the monomeric $[M(tmpyp)]^{4+}$ in aqueous solution and the $[M(tmpyp)]^{4+}$ molecules were seen to exist in an isolated form within the MPS nano-cavities. The structure of the ($[M(tmpyp)]^{4+}$–MPS)/(MV^{2+}–TNS) hybrid films could thus be established by SEM, XRD, absorption and emission analyses, as shown in Fig. 1.

UV and Visible Light Irradiation of the ($[H_2(tmpyp)]^{4+}$–MSP)/(MV^{2+}–TNS) Hybrid Films. The ($[H_2(tmpyp)]^{4+}$–MPS)/(MV^{2+}–TNS) composite film was irradiated for 3 h by visible light of 390–550 nm. The incident light was quantitatively absorbed by $[H_2(tmpyp)]^{4+}$ and no detectable changes

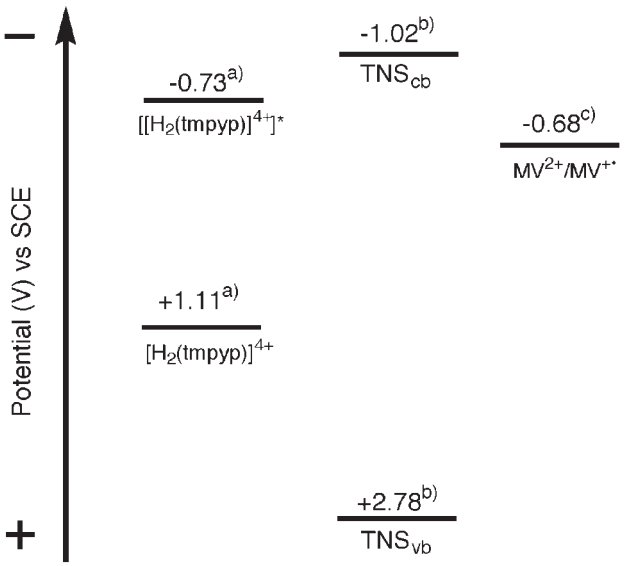

a) Ref. 36. b) Ref. 37. c) Ref. 40.

Scheme 2.

in the absorption spectra could be observed as judged by the endothermicity in the photoelectron transfer between the porphyrin and MV^{2+}, that is, TNS has a conduction band potential at −1.02 V (vs SCE),[35] which is more negative than the lowest excited redox potential of $[H_2(tmpyp)]^{4+}$, i.e., $[E^0(S^+/S^*)] = -0.73$ V (vs SCE),[36] as shown in Scheme 2.

In addition to visible light photolysis, UV light irradiation (270–380 nm) of the ($[H_2(tmpyp)]^{4+}$–MSP)/(MV^{2+}–TNS) films was carried out under these conditions and more than 99% of the incident UV light could be absorbed by TNS. Upon steady irradiation, the color of the ($[H_2(tmpyp)]^{4+}$–MSP)/(MV^{2+}–TNS) films changed from brown to blue, indicating the formation of one-electron reduced MV^{2+} ($MV^{+\bullet}$). The lifetime of $MV^{+\bullet}$ was extremely stable compared to other systems such as when $MV^{+\bullet}$ is incorporated in polymer matrices.[27] Nakato et al. have reported that for the photoinduced electron transfer between LMOS and MV^{2+}, the lifetime of $MV^{+\bullet}$ was strongly affected by the micro structure of the LMOS/MV^{2+} hybrids.[13a–h] In the present case, the short interlayer distance and flattened orientation of the MV^{2+} molecules within the TNS interlayers may have also resulted in the stabilization of $MV^{+\bullet}$. The 433 nm Soret absorption band diminished and new bands at 375 and around 600 nm were observed with two clear isosbestic points at ca. 400 and 472 nm, as shown in Fig. 4a. The formation of the bands at 375 and around 600 nm assigned to the one-electron reduced MV^{2+} ($MV^{+\bullet}$)[27,37–39] could be explained by the fact that TNS [−1.02 V (vs SCE)][35] has a more negative conduction band potential than the redox potential of the ground state of MV^{2+} [−0.68 V (vs SCE)],[40] and is thus exothermic for electron transfers (Scheme 2). Moreover, TNS has a positive valence band potential of +2.78 V (vs SCE),[35] which is more than the redox potential for the ground state of $[H_2(tmpyp)]^{4+}$ at +1.11 V (vs SCE),[36] so that the $[H_2(tmpyp)]^{4+}$ molecules were oxidatively decomposed by the holes (h^+) of the charge-separated TNS. Two clear isosbestic points at ca. 400

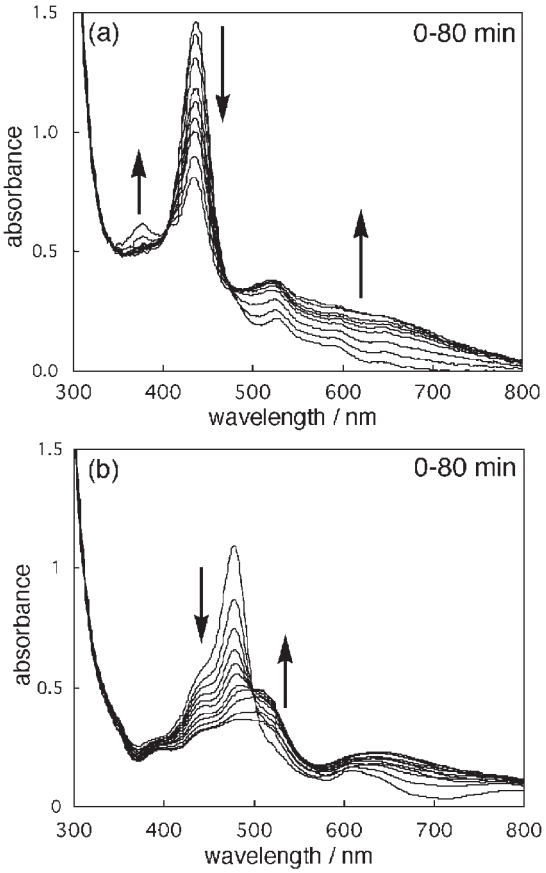

Fig. 4. Changes in the absorption spectra of: (a) the ($[H_2(tmpyp)]^{4+}$–MPS)/(MV^{2+}–TNS) film; (b) the (MPS)/($[H_2(tmpyp)]^{4+}$–TNS) film, upon UV light irradiation for 0–80 min.

and 472 nm were observed for the absorption spectra, indicating that the formation of $MV^{+\bullet}$ and the decomposition of $[H_2(tmpyp)]^{4+}$ occurred simultaneously.

A control experiment to confirm the electron accepting role of MV^{2+} in TNS was carried out. $[H_2(tmpyp)]^{4+}$ was intercalated in TNS but not in MPS, i.e., a (MPS)/($[H_2(tmpyp)]^{4+}$–TNS) thin film was prepared by casting MPS without MV^{2+} and then soaked in a $[H_2(tmpyp)]^{4+}$ solution. No adsorption of the $[H_2(tmpyp)]^{4+}$ molecules into the MPS nano-cavities could be confirmed by absorption measurements of the films. Upon UV irradiation, the absorption intensity of the Soret band decreased, although the changes in the absorption spectra for $[H_2(tmpyp)]^{4+}$ in (MPS)/($[H_2(tmpyp)]^{4+}$–TNS) were quite different than for those in the ($[H_2(tmpyp)]^{4+}$–MPS)/(MV^{2+}–TNS) films, as shown in Fig. 4b. The 475 nm Soret absorption band decreased and a new absorption band at around 450–550 nm appeared with an isosbestic point at 500 nm. The decomposition of $[H_2(tmpyp)]^{4+}$ in the (MPS)/($[H_2(tmpyp)]^{4+}$–TNS) system was seen to be completely different than for the ($[H_2(tmpyp)]^{4+}$–MPS)/(MV^{2+}–TNS) hybrids; thus, the $[H_2(tmpyp)]^{4+}$ molecules are considered to be decomposed by the electrons generated in the conduction band (e^-_{cb}) of TNS. These results suggest that photochemically formed holes in the valence band of the TNS were able to migrate to the $[H_2(tmpyp)]^{4+}$ molecules in the MPS nano-cavities. The reaction mechanism for the ($[H_2(tmpyp)]^{4+}$–MPS)/(MV^{2+}–TNS) film is proposed as follows:

$$TNS + h\nu\ (\text{UV-light}) \rightarrow e^-_{cb} + h^+, \quad (1)$$

$$e^-_{cb} + MV^{2+} \rightarrow MV^{+\bullet}, \quad (2)$$

$$h^+ + [H_2(tmpyp)]^{4+} \rightarrow \text{bleach}, \quad (3)$$

where e^-_{cb} and h^+ indicate an electron in the conduction band and a hole in the valence band of TNS, respectively.

The one-electron oxidation of $[H_2(tmpyp)]^{4+}$ must, nevertheless, be verified to be in conjunction with the one-electron reduction of MV^{2+} for TNS in the consecutively stacked MPS/TNS hybrid films. In order to substantiate the electron flow from $[H_2(tmpyp)]^{4+}$–MPS to the MV^{2+}–TNS hybrids, the following indirect evidence has been established in this study: (1) In the absence of TNS, UV-light irradiation of ($[H_2(tmpyp)]^{4+}$–MPS) did not cause decomposition of the $[H_2(tmpyp)]^{4+}$ film; (2) electric insulating polymers, such as poly(styrenes), poly(vinyl alcohols), or poly(ethylenes), sandwiched by the ($[H_2(tmpyp)]^{4+}$–MPS) and (MV^{2+}–TNS) hybrids suppressed the oxidative decomposition of $[H_2(tmpyp)]^{4+}$, but could still induce the formation of $MV^{+\bullet}$ under UV light irradiation; (3) after UV light irradiation followed by storage under dark conditions, the ($[H_2(tmpyp)]^{4+}$–MPS)/(MV^{2+}–TNS) films were able to recover the original Soret absorption band of $[H_2(tmpyp)]^{4+}$ accompanied by the disappearance of $MV^{+\bullet}$. A back electron transfer from $MV^{+\bullet}$ to the oxidized $[H_2(tmpyp)]^{4+}$ [$([H_2(tmpyp)]^{4+})_{ox}$] was thus observed. Further charge separation could be induced from the original $[H_2(tmpyp)]^{4+}$ and MV^{2+} pair, reversibly back and forth, upon alternating UV light irradiation and dark conditions. These results indicate the electron transfer and charge separation between the $[H_2(tmpyp)]^{4+}$ in the MPS cavities and the MV^{2+} within the interlayers of TNS, although the mechanisms behind these reactions have yet to be clarified. However, the adsorbed water molecules or oxygen may assist this unique photoinduced electron transfer observed between $[H_2(tmpyp)]^{4+}$ and MV^{2+}. More detailed investigations such as kinetic analyses of the force and back electron transfers, photoreactions under vacuo, oxygen, and water-saturated conditions, and the modification of the TNS/MPS interfaces are now underway.

Effect of the Hole-Restoration Reagents. The oxidative decomposition of the $[H_2(tmpyp)]^{4+}$ molecules in the MPS nano-cavities by the holes of TNS (h^+) was confirmed by incorporating hole-restoration reductants to recover the one-electron oxidized $[H_2(tmpyp)]^{4+}$ in the MPS nano-cavities.[5a,b,41] Two different types of hole-restoration agents, hydroquinone (HQ: oxidation potential = +0.21 V vs SCE)[42,43] and methylene blue (MB: oxidation potential = +0.29 V vs SCE), were employed.[43] The changes observed in the absorption spectra of [(HQ + $[H_2(tmpyp)]^{4+}$)–MPS]/(MV^{2+}–TNS) and [(MB + $[H_2(tmpyp)]^{4+}$)–MPS]/(MV^{2+}–TNS) are shown in Figs. 5a and 5b, respectively.

HQ, a hole-restoration agent, was used to detect $MV^{+\bullet}$ (λ_{max} = 375 and around 600 nm) due to its transparency in regions longer than 350 nm. Under UV light irradiation, the formation of $MV^{+\bullet}$ could easily be detected in the [(HQ + $[H_2(tmpyp)]^{4+}$)–MPS]/(MV^{2+}–TNS) hybrid and the yield was similar to that for the ($[H_2(tmpyp)]^{4+}$–MPS)/(MV^{2+}–TNS) films without HQ, as shown in Figs. 5a and 4a, respec-

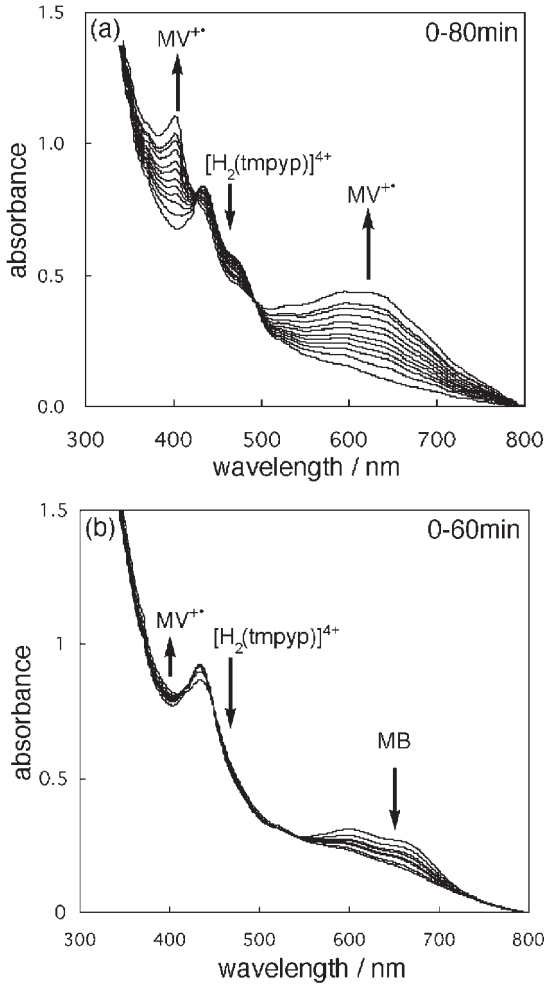

Fig. 5. Changes in the absorption spectra for: (a) the [(HQ + $[H_2(tmpyp)]^{4+}$)–MPS]/(MV^{2+}–TNS) film; and (b) the [(MB + $[H_2(tmpyp)]^{4+}$)–MPS]/(MV^{2+}–TNS) film, upon UV light irradiation.

tively. However, due to spectral overlapping with TNS, the decomposition of HQ could not be confirmed. In place of HQ, MB was employed as the hole-restoration agent, and in the run with MB, the spectral changes for MB (decomposed by h^+) were clearly observed, although the formation of $MV^{+\bullet}$ could not be detected in the range of 550–750 nm. In the photolysis together with MB, the spectral changes in visible light regions overlapped with the absorption of the $MV^{+\bullet}$ yield, making it difficult to follow the spectral changes for the formation of $MV^{+\bullet}$. However, upon UV light irradiation of the [(MB + $[H_2(tmpyp)]^{4+}$)–MPS]/(MV^{2+}–TNS) films (Fig. 5b), two diminishing absorption bands at around 433 and 550–750 nm appeared, then a weak absorption at around 400 nm appeared in their place. The decrease in the absorption intensities at 433 and 550–750 nm corresponded with the decomposition of $[H_2(tmpyp)]^{4+}$ and MB, respectively, while the increase at 400 nm could be assigned to the formation of $MV^{+\bullet}$. These results indicate that the electron transfer of e^-_{cb} to MV^{2+} is accompanied by a 80–90% decomposition of $[H_2(tmpyp)]^{4+}$ without the hole-restoration agents in the MPS nano-cavities. However, the decomposition of the $[H_2(tmpyp)]^{4+}$ molecules was seen to be suppressed to 2–3% by the addition of either

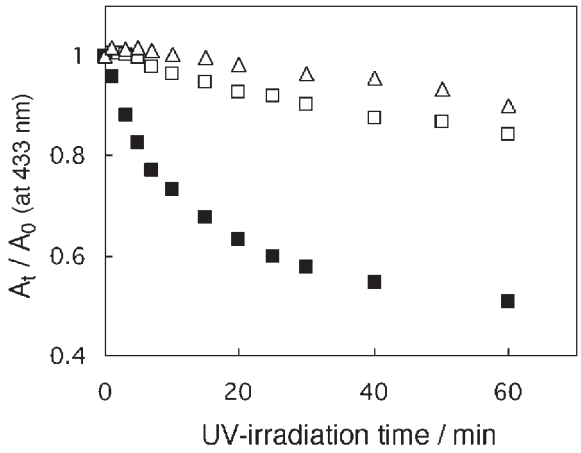

Fig. 6. Changes in the relative absorption intensity (A_t/A_0) at a Soret maxima of 433 nm for the $[H_2(tmpyp)]^{4+}$ in ($[H_2(tmpyp)]^{4+}$–MPS)/(MV^{2+}–TNS) hybrid film as a function of the UV light irradiation time. Solid square: without restoration reagents and only $[H_2(tmpyp)]^{4+}$; Open square: HQ; Open triangle: MB co-existing with $[H_2(tmpyp)]^{4+}$ in the MPS nano-cavities.

HQ or MB as the hole-restoration agent. Figure 6 shows the changes in the normalized Soret absorption intensity (A_t/A_0 at 433 nm) against the UV light irradiation time both in the presence and absence of HQ or MB. A clear suppression against the decomposition of $[H_2(tmpyp)]^{4+}$ in the MPS nano-cavities can be observed for both HQ and MB. HQ and MB were thus seen to work as reductants for the holes of TNS (h^+) or the oxidized species of $[H_2(tmpyp)]^{4+}$ [$([H_2(tmpyp)]^{4+})_{ox}$], leading to the conclusion that the decomposition of $[H_2(tmpyp)]^{4+}$ proceeds through oxidation processes, even when $[H_2(tmpyp)]^{4+}$ molecules are adsorbed onto the MPS nano-cavities. Also, by using two types of hole-restoration agents, HQ or MB, the disadvantages of either could be complemented.

Visible Light-Induced Electron Transfer Using [Zn(tmpyp)]$^{4+}$ or [Co(tmpyp)]$^{4+}$ in the (MPS)/(MV^{2+}–TNS) Hybrid Films. Although $[H_2(tmpyp)]^{4+}$ could initiate UV light-induced electron transfers in the ($[H_2(tmpyp)]^{4+}$–MPS)/(MV^{2+}–TNS) hybrid films, visible light-induced electron transfers could not be observed since TNS has a more negative conduction band potential than the redox potential in the excited state for $[H_2(tmpyp)]^{4+}$. To address this concern, $[Zn(tmpyp)]^{4+}$ and $[Co(tmpyp)]^{4+}$ were used in place of $[H_2(tmpyp)]^{4+}$, since they have a more negative redox potential than $[H_2(tmpyp)]^{4+}$;[36,44] and in fact, visible light-induced electron transfers could then be observed in the stacked thin films, as shown in Scheme 3.

The electron transfers within the MPS/TNS hybrid films were first confirmed by UV light irradiation for the ([Zn(tmpyp)]$^{4+}$ or $[Co(tmpyp)]^{4+}$–MPS)/(MV^{2+}–TNS) hybrid films. Upon UV light irradiation, a decrease in the Soret absorption peak accompanied by an increase in the absorption of $MV^{+\bullet}$ was observed with two isosbestic points (data not shown), as can be seen in Fig. 4a, indicating that photoinduced electron transfers could in fact take place in the present hybrid films.

The ($[Zn(tmpyp)]^{4+}$–MPS)/(MV^{2+}–TNS) hybrid films were irradiated with visible light of 390–550 nm, inducing

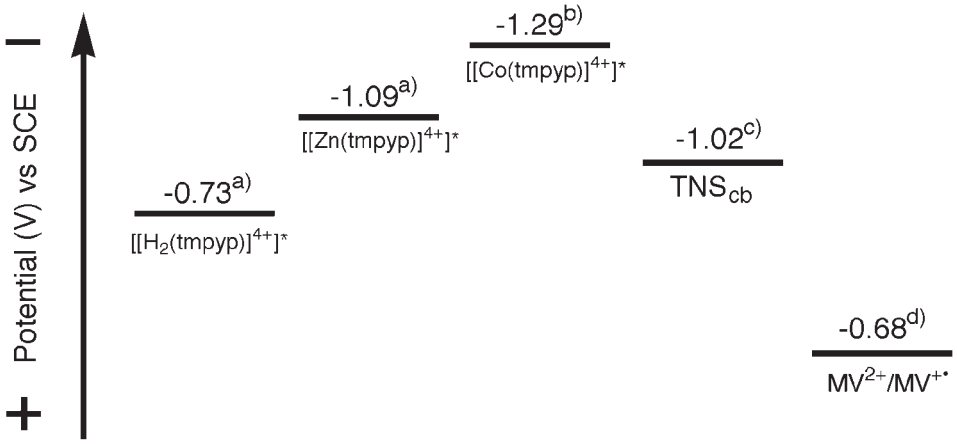

a) Ref. 36. b) Ref. 44. c) Ref. 35. d) Ref. 40.

Scheme 3.

the exclusive excitation of $[M(tmpyp)]^{4+}$. A decrease in the Soret absorption peak for $[Zn(tmpyp)]^{4+}$ and an increase in the broad absorption peak of 550–750 nm could be simultaneously observed, as shown in Fig. 7a. An increase in the broad absorption at 550–750 nm corresponded with the formation of $MV^{+\bullet}$. Similar spectral changes for the ($[Co(tmpyp)]^{4+}$–MPS)/(MV^{2+}–TNS) hybrid films upon irradiation by visible light are shown in Fig. 7b. $[Zn(tmpyp)]^{4+}$ and $[Co(tmpyp)]^{4+}$ possess excited redox potentials of −1.09 V (vs SCE)[36] and −1.29 V (vs SCE),[44] respectively, which are more negative than the conduction band potential for TNS (Scheme 3). Exothermic electron transfers were, therefore seen to take place by visible light irradiation of $[Zn(tmpyp)]^{4+}$ or $[Co(tmpyp)]^{4+}$, as depicted in the following equations:

$$[M(tmpyp)]^{4+} + h\nu \text{ (vis-light)} \rightarrow ([M(tmpyp)]^{4+})^*, \quad (4)$$

$$([M(tmpyp)]^{4+})^* + TNS \rightarrow ([M(tmpyp)]^{4+})_{ox} + e^-_{cb}, \quad (5)$$

$$e^-_{cb} + MV^{2+} \rightarrow MV^{+\bullet}, \quad (6)$$

$$([M(tmpyp)]^{4+})_{ox} \rightarrow \text{bleach}, \quad (7)$$

where M in $[M(tmpyp)]^{4+}$ denotes the Zn or Co atoms. The electrons migrate from the excited $[M(tmpyp)]^{4+}$ to the TNS conduction band, while a one-electron oxidized species of $[M(tmpyp)]^{4+}$ ($[([M(tmpyp)]^{4+})_{ox}]$ was formed along with the generation of electrons in the conduction band of TNS (e^-_{cb}), as shown in Eq. 5. The e^-_{cb} then migrated to the ground state of MV^{2+} to form the reduction product of MV^{2+} ($MV^{+\bullet}$) (Eq. 6), so that during irradiation $([M(tmpyp)]^{4+})_{ox}$ was seen to be bleached of color due to decomposition (Eq. 7).

Conclusion

In this work, integrated hybrid films of two spatially different nano-structured materials, titania nanosheets (TNS) and mesoporous silica (MPS), were successfully synthesized. SEM and XRD analyses showed the MPS and TNS films to be independently stacked on the substrate. In addition, guest metalloporphyrins ($[M(tmpyp)]^{4+}$; M = H_2, Zn, and Co) could be adsorbed into the host MPS nano-cavities and MV^{2+} into the interlayers of TNS, separately and selectively. Absorption measurements also confirmed the separate accommodation of

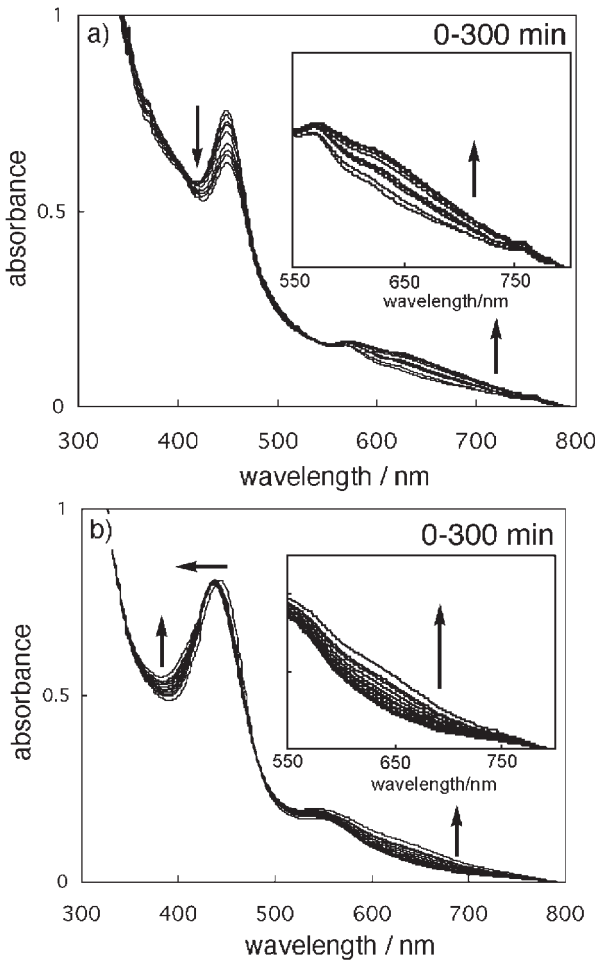

Fig. 7. Changes in the absorption spectra of: (a) the ($[Zn(tmpyp)]^{4+}$–MPS)/(MV^{2+}–TNS) and; (b) the ($[Co(tmpyp)]^{4+}$–MPS)/(MV^{2+}–TNS) films upon visible light irradiation for 0–300 min. Inset shows an expansion at 550–800 nm regions.

$[M(tmpyp)]^{4+}$ into the MPS nano-cavities and the adsorption of MV^{2+} onto the TNS layers, that is, under the present experimental conditions, $[M(tmpyp)]^{4+}$ and MV^{2+} could be selectively and separately confined by the alternately stacked TNS/MPS hybrid thin films.

Upon UV light irradiation and excitation of TNS in the ($[H_2(tmpyp)]^{4+}$–MPS)/(MV^{2+}–TNS) films, the decomposition of $[H_2(tmpyp)]^{4+}$ and the formation of a one-electron reductant of MV^{2+} ($MV^{+\bullet}$) were simultaneously observed, indicating that TNS could operate as an effective photocatalyst. Also, in order to confirm the role of $[H_2(tmpyp)]^{4+}$ as a hole-restoration agent, reductants such as HQ or MB were co-adsorbed into the MPS nano-cavities with $[H_2(tmpyp)]^{4+}$ followed by UV light irradiation. The decomposition of the $[H_2(tmpyp)]^{4+}$ molecules was seen to be suppressed, indicating that they were oxidized by the holes of TNS and then bleached of color. These results clearly show that hole transfers could take place in these MPS/TNS hybrid films.

In further studies, the hybrids ($[H_2(tmpyp)]^{4+}$–MPS)/(MV^{2+}–TNS) were modified with metal complex $[M(tmpyp)]^{4+}$ (M = Zn or Co), i.e., $[Zn(tmpyp)]^{4+}$ or $[Co(tmpyp)]^{4+}$. Upon visible light irradiation, the formation of $MV^{+\bullet}$ and the decomposition of $[M(tmpyp)]^{4+}$ were clearly observed, showing that visible light-induced electron transfers could proceed on these MPS/TNS hybrid films, the first report of such charge separation in consecutively stacked thin films by both UV and visible light.

This work was partly supported by a Grant-in-Aid for Scientific Research on Priority Areas (417) of the Ministry of Education, Culture, Sports, Science and Technology (MEXT) of Japan. We would like to thank them for their kind assistance. Sincere thanks are also extended to CREST (Core Research for Evolutional Science and Technology) of JST (Japan Science and Technology Corporation) for their valuable support.

References

1 *Bunshininshiki-Kagaku*, ed. by H. Tsukube, Sankyo-Shuppan, Tokyo, **1997**.

2 M. Senoo, K. Araki, J. Ohotsuki, *Choubunshi-Kagaku*, Tokyo Kagaku Doujin, Tokyo, **1998**.

3 a) D. W. Breck, *Zeolite Molecular Sieves*, Wiley, New York, **1974**. b) N. Y. Chen, W. E. Garwood, F. G. Dwyer, *Shape Selective Catalysis in Industrial Applications*, Marcel Dekker, New York, **1989**.

4 V. Ramamurthy, *J. Photochem. Photobiol., C* **2000**, *1*, 145.

5 a) T. Itoh, K. Yano, Y. Inada, Y. Fukushima, *J. Mater. Chem.* **2002**, *12*, 3275. b) T. Itoh, K. Yano, Y. Inada, Y. Fukushima, *J. Am. Chem. Soc.* **2002**, *124*, 13437. c) A. Corma, *Chem. Rev.* **1997**, *97*, 710. d) C. T. Kresge, M. E. Leonowick, W. J. Roth, J. C. Vartuli, J. S. Beck, *Nature* **1992**, *359*, 710. e) J. S. Beck, J. C. Vartuli, W. J. Roth, M. E. Leonowicz, C. T. Kresge, K. D. Schmitt, C. T.-W. Chu, D. H. Olson, E. W. Sheppard, S. B. McCullen, J. B. Higgins, J. L. Schlenkert, *J. Am. Chem. Soc.* **1992**, *114*, 10834. f) S. Oliver, A. Kuperaman, N. Coombs, A. Lough, G. Ozin, *Nature* **1995**, *378*, 47. g) M. Yada, M. Machida, T. Kijima, *J. Chem. Soc., Chem. Commun.* **1996**, 769. h) S. Inagaki, Y. Fukushima, K. Kuroda, *J. Chem. Soc., Chem. Commun.* **1993**, 680. i) M. Ogawa, *J. Am. Chem. Soc.* **1994**, *116*, 7941. j) M. Ogawa, *J. Chem. Soc., Chem. Commun.* **1996**, 1149. k) M. Ogawa, *Langmuir* **1997**, *13*, 1853. l) M. Ogawa, T. Igarashi, K. Kuroda, *Bull. Chem. Soc. Jpn.* **1997**, *70*, 2833. m) M. Ogawa, *Langmuir* **1995**, *11*, 4639. n) A. Yoshida, N. Kakegawa, M. Ogawa, *Res. Chem. Intermed.* **2003**, *29*, 721.

6 M. Ogawa, *J. Photochem. Photobiol., C* **2002**, *3*, 129.

7 a) B. K. G. Theng, *The Chemistry of Clay-Organic Reactions*, Adam Hilger, London, **1974**; H. van Olphen, *An Introduction to Clay Colloid Chemistry*, 2nd ed., Wiley-Interscience, New York, **1977**; H. Shiramizu, *Clay Mineralogy*, Asakura-shoten, Tokyo, **1988**.

8 a) M. Ogawa, K. Kuroda, *Chem. Rev.* **1995**, *95*, 399. b) M. Ogawa, K. Kuroda, *Bull. Chem. Soc. Jpn.* **1997**, *70*, 2593.

9 a) *Science and Applications of Inorganic Nanosheets*, ed. by K. Kuroda, T. Sasaki, NTS, Tokyo, **2005**. b) K. Takagi, T. Shichi, *Solid State and Surface Photochemistry*, ed. by V. Ramamurthy, K. Schanze, Marcel Dekker, New York, **2000**, Vol. 5, p. 31. c) T. Shichi, K. Takagi, *J. Photochem. Photobiol., C.* **2000**, *1*, 113. d) T. Yui, K. Takagi, *J. Soc. Photogr. Sci. Technol. Jpn.* **2003**, *66*, 326.

10 a) T. Itoh, T. Shichi, T. Yui, H. Takahashi, Y. Inui, K. Takagi, *J. Phys. Chem. B* **2005**, *109*, 3199. b) M. Gelfer, C. Burger, A. Fadeev, I. Sics, B. Chu, B. S. Hsiao, A. Heintz, S.-L. Hsu, K. Kojo, M. Si, M. Rafailovich, *Langmuir* **2004**, *20*, 3746. c) I. Shindachi, H. Hanaki, R. Sasai, T. Shichi, T. Yui, K. Takagi, *Chem. Lett.* **2004**, *33*, 1116. d) M. Sumitani, S. Takagi, Y. Tanamura, H. Inoue, *Anal. Sci.* **2004**, *20*, 1153. e) T. Itoh, N. Ohta, T. Shichi, T. Yui, K. Takagi, *Langmuir* **2003**, *19*, 9120. f) L. A. Lucia, T. Yui, R. Sasai, H. Yoshida, S. Takagi, K. Takagi, D. G. Whitten, H. Inoue, *J. Phys. Chem. B* **2003**, *107*, 3789. g) T. Yui, R. A. Sundara, T. Shimada, H. Yoshida, D. A. Tryk, H. Inoue, *Langmuir* **2002**, *18*, 4232. h) T. Yui, H. Yoshida, H. Tachibana, D. A. Tryk, H. Inoue, *Langmuir* **2002**, *18*, 891. i) R. Matsuoka, T. Yui, R. Sasai, K. Takagi, H. Inoue, *Mol. Cryst. Liq. Cryst.* **2000**, *341*, 1137. j) T. Itoh, T. Shichi, T. Yui, K. Takagi, *Langmuir* **2005**, *21*, 3217. k) T. Itoh, M. Yamashita, T. Shichi, T. Yui, K. Takagi, *Chem. Lett.* **2005**, *34*, 990. l) T. Shiragami, K. Nabeshima, M. Yasuda, H. Inoue, *Chem. Lett.* **2003**, *32*, 148. m) T. Shiragami, K. Nabeshima, J. Matsumoto, M. Yasuda, H. Inoue, *Chem. Lett.* **2003**, *32*, 484. n) T. Yui, I. Shindachi, R. Sasai, K. Takagi, *Mol. Cryst. Liq. Cryst.* **2005**, *431*, 321. o) V. M. Martinez, F. L. Arbeloa, J. B. Prieto, I. L. Arbeloa, *J. Phys. Chem. B* **2005**, *109*, 7443. p) R. Sasai, T. Fujita, N. Iyi, H. Itoh, K. Takagi, *Langmuir* **2002**, *18*, 6578. q) R. Sasai, N. Iyi, T. Fujita, K. Takagi, H. Itoh, *Chem. Lett.* **2003**, *32*, 550. r) R. Sasai, N. Iyi, T. Fujita, F. L. Arbeloa, V. M. Martinez, K. Takagi, H. Itoh, *Langmuir* **2004**, *20*, 4715. s) R. Sasai, D. Sugiyama, S. Takahashi, Z. Tong, T. Shichi, H. Itoh, K. Takagi, *J. Photochem. Photobiol., A* **2003**, *155*, 223. t) M. Sumitani, Y. Tanamura, T. Hiratani, T. Ohmachi, H. Inoue, *J. Phys. Chem. Solids* **2005**, *66*, 1228. u) T. Itoh, T. Shichi, T. Yui, K. Takagi, *J. Colloid Interface Sci.* **2005**, *291*, 218.

11 Y. Yamaguchi, T. Yui, S. Takagi, T. Shimada, H. Inoue, *Chem. Lett.* **2001**, 644; M. A. Bizeto, D. L. A. de Faria, V. R. L. Constantino, *J. Mater. Sci.* **2002**, *37*, 265; M. A. Bizeto, V. R. L. Constantino, *Mater. Res. Bull.* **2004**, *39*, 1729; M. A. Bizeto, V. R. L. Constantino, *Mater. Res. Bull.* **2004**, *39*, 1811; M. A. Bizeto, V. R. L. Constantino, *Microporous Mesoporous Mater.* **2005**, *83*, 212.

12 K. Yao, S. Nishimura, Y. Imai, H. Wang, T. Ma, E. Abe, H. Tateyama, A. Yamagishi, *Langmuir* **2003**, *19*, 321; N. Miyamoto, K. Kuroda, M. Ogawa, *J. Phys. Chem. B* **2004**, *108*, 2468; G. B. Saupe, T. E. Mallouk, W. Kim, R. H. Schmehl,

J. Phys. Chem. B **1997**, *101*, 2508; Y. I. Kim, S. J. Atherton, E. S. Brigham, T. E. Mallouk, *J. Phys. Chem.* **1993**, *97*, 11802; Y. I. Kim, S. Salim, M. J. Huq, T. E. Mallouk, *J. Am. Chem. Soc.* **1991**, *113*, 9561; S. W. Keller, S. A. Johnson, E. S. Brigham, E. H. Yonemoto, T. E. Mallouk, *J. Am. Chem. Soc.* **1995**, *117*, 12879; D. L. Feldheim, K. C. Grabar, M. J. Natan, T. E. Mallouk, *J. Am. Chem. Soc.* **1996**, *118*, 7640; M. Fang, D. M. Kaschak, A. C. Sutorik, T. E. Mallouk, *J. Am. Chem. Soc.* **1997**, *119*, 12184; D. M. Kaschak, J. T. Lean, C. C. Waraksa, G. B. Saupe, H. Usami, T. E. Mallouk, *J. Am. Chem. Soc.* **1999**, *121*, 3435; H. Usami, T. Itakura, A. Nakasa, E. Suzuki, *J. Chem. Eng. Jpn.* **2005**, *38*, 664.

13 a) T. Nakato, K. Kuroda, C. Kato, *J. Chem. Soc., Chem. Commun.* **1989**, 1144. b) T. Nakato, K. Kuroda, C. Kato, *Chem. Mater.* **1992**, *4*, 128. c) T. Nakato, H. Miyata, K. Kuroda, C. Kato, *React. Solids* **1988**, *6*, 231. d) T. Nakato, K. Kuroda, *Eur. J. Solid State Inorg. Chem.* **1995**, *32*, 809. e) T. Nakato, K. Kusunoki, K. Yoshizawa, K. Kuroda, M. Kaneko, *J. Phys. Chem.* **1995**, *99*, 17896. f) R. Shinozaki, T. Nakato, *Langmuir* **2004**, *20*, 7583. g) T. Nakato, D. Sakamoto, K. Kuroda, C. Kato, *Bull. Chem. Soc. Jpn.* **1992**, *65*, 322. h) T. Nakato, H. Miyashita, S. Yakabe, *Chem. Lett.* **2003**, *32*, 72. i) A. Furube, T. Shiozawa, A. Ishikawa, A. Wada, K. Domen, C. Hirose, *J. Phys. Chem. B* **2002**, *106*, 3065.

14 T. Hattori, Y. Sugito, T. Yui, K. Takagi, *Chem. Lett.* **2005**, *34*, 1074; Z. Tong, T. Shichi, Y. Kasuga, K. Takagi, *Chem. Lett.* **2002**, *34*, 1206; Z. Tong, G. Zhang, S. Takagi, T. Shimada, H. Tachibana, H. Inoue, *Chem. Lett.* **2005**, *34*, 632; Z. Tong, S. Takagi, H. Tachibana, K. Takagi, H. Inoue, *Chem. Lett.* **2005**, *34*, 608; Z. Tong, S. Takagi, T. Shimada, H. Tachibana, H. Inoue, *Chem. Lett.* **2005**, *34*, 1406; Z. Tong, S. Takagi, H. Tachibana, K. Takagi, H. Inoue, *J. Phys. Chem. B* **2005**, *109*, 21612; Z. Tong, S. Takagi, T. Shimada, H. Tachibana, H. Inoue, *J. Am. Chem. Soc.* **2006**, *128*, 684.

15 a) Z. Tong, T. Shichi, K. Oshika, K. Takagi, *Chem. Lett.* **2002**, 876. b) Z. Tong, T. Shichi, K. Takagi, *J. Phys. Chem. B* **2002**, *106*, 13306.

16 *The Porphyrin Handbook*, ed. by K. M. Kadish, K. M. Smith, R. Guilard, Academic Press, New York, **1999**; S. Takagi, H. Inoue, *Multimetallic and Macromolecular Inorganic Photochemistry*, ed. by V. Ramamurthy, K. S. Schanze, Marcel Dekker, New York, **2000**, Vol. 6, p. 215.

17 H. Inoue, M. Sumitani, A. Sekita, M. Hida, *J. Chem. Soc., Chem. Commun.* **1987**, 1681; H. Inoue, T. Okamoto, Y. Kameo, M. Sumitani, A. Fujiwara, D. Ishibashi, M. Hida, *J. Chem. Soc., Perkin Trans. 1* **1994**, 105; T. Okamoto, S. Takagi, T. Shiragami, H. Inoue, *Chem. Lett.* **1993**, 687; S. Takagi, T. Okamoto, T. Shiragami, H. Inoue, *J. Org. Chem.* **1994**, *59*, 7373; T. Shiragami, K. Kubomura, D. Ishibashi, H. Inoue, *J. Am. Chem. Soc.* **1996**, *118*, 6311; S. Takagi, M. Suzuki, T. Shiragami, H. Inoue, *J. Am. Chem. Soc.* **1997**, *119*, 8712; H. Inoue, S. Funyu, Y. Shimada, S. Takagi, *Pure Appl. Chem.* **2005**, *77*, 1019; S. Funyu, T. Isobe, S. Takagi, H. Inoue, *J. Am. Chem. Soc.* **2003**, *125*, 5734.

18 D. M. Togashi, S. M. B. Costa, *New J. Chem.* **2002**, *26*, 1774; E. A. Malinka, A. M. Khutornoi, S. V. Vodzinskii, Z. I. Zhilina, G. L. Kamalov, *React. Kinet. Catal. Lett.* **1998**, *36*, 407; P. M. R. Paulo, S. M. B. Costa, *J. Phys. Chem. B* **2005**, *109*, 13928; P. M. R. Paulo, S. M. B. Costa, *Photochem. Photobiol. Sci.* **2003**, *2*, 597; P. M. R. Paulo, R. Gronheid, F. C. De Schryver, S. M. B. Costa, *Macromolecules* **2003**, *36*, 9135; Z. Varpness, J. W. Peters, M. Young, T. Douglas, *Nano Lett.* **2005**, *5*, 2306.

19 M. Grätzel, *Nature* **2001**, *414*, 338; M. Grätzel, *J. Photochem. Photobiol., C* **2003**, *4*, 145; K. Kalyanasundaram, N. Vlachopoulos, V. Krishnan, A. Monnier, M. Grätzel, *J. Phys. Chem.* **1987**, *91*, 2342.

20 A. Brune, G. Jeong, P. A. Liddell, T. Sotomura, T. A. Moore, A. L. Moore, D. Gust, *Langmuir* **2004**, *20*, 8366; P. V. Kamat, *J. Phys. Chem.* **1989**, *93*, 859.

21 T. Sasaki, M. Watanabe, H. Hashizume, H. Yamada, H. Nakazawa, *J. Chem. Soc., Chem. Commun.* **1996**, 229; T. Sasaki, M. Watanabe, *J. Am. Chem. Soc.* **1998**, *120*, 4682.

22 T. Sasaki, Y. Ebina, T. Tanaka, M. Watanabe, G. Decher, *J. Chem. Soc., Chem. Commun.* **2000**, 2163.

23 T. Sasaki, M. Watanabe, H. Hashizume, H. Yamada, H. Nakazawa, *J. Am. Chem. Soc.* **1996**, *118*, 8329.

24 T. Sasaki, Y. Ebina, T. Tanaka, M. Harada, M. Watanabe, *Chem. Mater.* **2001**, *13*, 466; L. Z. Wang, T. Sasaki, Y. Ebina, K. Kurashima, M. Watanabe, *Chem. Mater.* **2002**, *14*, 4827; T. Sasaki, Y. Ebina, K. Fukuda, T. Tanaka, M. Harada, M. Watanabe, *Chem. Mater.* **2002**, *14*, 3524.

25 L. Wang, Y. Omomo, N. Sakai, K. Fukuda, I. Nakai, Y. Ebina, K. Takada, M. Watanabe, T. Sasaki, *Chem. Mater.* **2003**, *15*, 2873; L. Wang, K. Takada, A. Kajiyama, M. Onoda, Y. Michiue, L. Zhang, M. Watanabe, T. Sasaki, *Chem. Mater.* **2003**, *15*, 4508; F. F. Xu, Y. Ebina, Y. Bando, T. Sasaki, *J. Phys. Chem. B* **2003**, *107*, 9638; F. F. Xu, Y. Ebina, Y. Bando, T. Sasaki, *J. Phys. Chem. B* **2002**, *107*, 6698; M. Gateshki, S.-J. Hwang, D. H. Park, Y. Ren, V. Petkov, *Chem. Mater.* **2004**, *16*, 5153.

26 M. Muramatsu, K. Akatsuka, Y. Ebina, K. Wang, T. Sasaki, T. Ishida, K. Miyake, M. Haga, *Langmuir* **2005**, *21*, 6590; K. Saruwatari, H. Sato, T. Idei, J. Kameda, A. Yamagishi, A. Takagi, K. Domen, *J. Phys. Chem. B* **2005**, *109*, 12410; A. Takagi, M. Sugisawa, D. Lu, J. N. Kondo, M. Hara, K. Domen, S. Hayashi, *J. Am. Chem. Soc.* **2003**, *125*, 5479; T. Nakato, N. Miyamoto, A. Harada, *J. Chem. Soc., Chem. Commun.* **2004**, 78; K. Saruwatari, H. Sato, J. Kameda, A. Yamagishi, K. Domen, *J. Chem. Soc., Chem. Commun.* **2005**, 1999.

27 T. Yui, Y. Mori, T. Tsuchino, T. Itoh, T. Hattori, Y. Fukushima, K. Takagi, *Chem. Mater.* **2005**, *17*, 206.

28 a) T. Yui, T. Tsuchino, T. Itoh, M. Ogawa, Y. Fukushima, K. Takagi, *Langmuir* **2005**, *21*, 2644. b) T. Tachikawa, T. Yui, M. Fujitsuka, K. Takagi, T. Majima, *Chem. Lett.* **2005**, *34*, 1522.

29 J. P. Maier, F. Thommen, *J. Chem. Soc., Faraday Trans. 2* **1981**, *77*, 845.

30 M. Yuasa, T. Nagaiwa, T. Kato, I. Sekine, S. Hayashi, *J. Electrochem. Soc.* **1995**, *142*, 2612.

31 a) M. Ogawa, N. Masukawa, *Microporous Mesoporous Mater.* **2000**, *38*, 35. b) J. Y. Bae, O.-H. Park, J.-I. Jung, K. T. Ranjit, B.-S. Bae, *Microporous Mesoporous Mater.* **2004**, *67*, 265.

32 V. G. Kuykendall, J. K. Thomas, *Langmuir* **1990**, *6*, 1350; Z. Chernia, D. Gili, *Langmuir* **1999**, *15*, 1625.

33 a) M. Eguchi, S. Takagi, H. Tachibana, H. Inoue, *J. Phys. Chem. Solids* **2004**, *65*, 403. b) S. Takagi, T. Shimada, M. Eguchi, T. Yui, H. Yoshida, D. A. Tryk, H. Inoue, *Langmuir* **2002**, *18*, 2265. c) S. Takagi, T. Shimada, T. Yui, H. Inoue, *Chem. Lett.* **2001**, 128. d) M. Eguchi, S. Takagi, H. Inoue, *Chem. Lett.* **2006**, *35*, 14.

34 S. Takagi, D. A. Tryk, H. Inoue, *J. Phys. Chem. B* **2002**, *106*, 5455; S. Takagi, M. Eguchi, D. A. Tryk, H. Inoue, *Langmuir* **2006**, *22*, 1406.

35 N. Sakai, Y. Ebina, K. Takada, T. Sasaki, *J. Am. Chem. Soc.* **2004**, *126*, 5851.

36 K. Kalyanasundaram, M. Neumann-Spallart, *J. Phys. Chem.* **1982**, *86*, 5163; P. Worthington, R. F. X. Hambright, J. Williams, C. Reid, P. Burnham, J. Shamin, D. M. Turray, R. Bell, P. Kirkland, R. G. Little, N. Dutta-Gupta, U. Eisner, *J. Inorg. Biochem.* **1980**, *12*, 281.

37 H. Kamogawa, H. Mizuno, Y. Todo, M. Nagasawa, *J. Polym. Sci.* **1979**, *17*, 3149.

38 C. Lee, Y. M. Lee, M. S. Moon, S. H. Park, J. W. Park, K. G. Kim, S.-J. Jeon, *J. Electroanal. Chem.* **1996**, *416*, 139.

39 P. M. S. Monk, R. D. Fairweather, M. D. Ingram, J. A. Duffy, *J. Chem. Soc., Perkin Trans. 2* **1992**, 2039.

40 W. M. Clark, *Oxidation–Reduction Potentials of Organic Systems*, Robert E. Krieger Publishing Company, New York, **1972**.

41 T. Itoh, K. Yano, T. Kajino, S. Itoh, Y. Shibata, H. Mino, R. Miyamoto, Y. Inada, S. Iwai, Y. Fukushima, *J. Phys. Chem. B* **2004**, *108*, 13683.

42 Z. Chernia, D. Gill, *Langmuir* **1999**, *15*, 1625.

43 *Encyclopedia of Electrochemistry of the Elements*, ed. by A. J. Bard, H. Lund, Marcel Dekker, New York, **1973**, Vol. 9.

44 K. Yamamoto, S. Nakazawa, A. Matsufuji, T. Taguchi, *J. Chem. Soc., Dalton Trans.* **2001**, 251.